

<https://helda.helsinki.fi>

---

## MYC-Induced miR-203b-3p and miR-203a-3p Control Bc1-xL Expression and Paclitaxel Sensitivity in Tumor Cells

Aakko, Sofia

2019-01

---

Aakko , S , Straume , A H , Birkeland , E E , Chen , P , Qiao , X , Lonning , P E & Kallio , M J  
2019 , ' MYC-Induced miR-203b-3p and miR-203a-3p Control Bc1-xL Expression and  
Paclitaxel Sensitivity in Tumor Cells ' , Translational oncology , vol. 12 , no. 1 , pp. 170-179 . <https://doi.org/10.1016/j>

---

<http://hdl.handle.net/10138/287674>

<https://doi.org/10.1016/j.tranon.2018.10.001>

---

cc\_by\_nc\_nd

publishedVersion

---

*Downloaded from Helda, University of Helsinki institutional repository.*

*This is an electronic reprint of the original article.*

*This reprint may differ from the original in pagination and typographic detail.*

*Please cite the original version.*

## MYC-Induced miR-203b-3p and miR-203a-3p Control Bcl-xL Expression and Paclitaxel Sensitivity in Tumor Cells<sup>1</sup>



Sofia Aakko<sup>\*,†</sup>, Anne Hege Straume<sup>‡,§</sup>, Einar Elvbakken Birkeland<sup>‡,§</sup>, Ping Chen<sup>¶, #</sup>, Xi Qiao<sup>†</sup>, Per Eystein Lønning<sup>‡,§</sup> and Marko J. Kallio<sup>\*,†</sup>

\*Institute of Biomedicine, Research Centre for Integrative Physiology and Pharmacology, University of Turku, 20520 Turku, Finland; <sup>†</sup>Turku Centre for Biotechnology, University of Turku and Åbo Akademi University, 20520 Turku, Finland; <sup>‡</sup>Department of Clinical Science, University of Bergen, 5020 Bergen, Norway; <sup>§</sup>Department of Clinical Oncology, Haukeland University Hospital, 5020 Bergen, Norway; <sup>¶</sup>Research Programs Unit, Genome-Scale Biology, Faculty of Medicine, University of Helsinki, 00014, Helsinki, Finland; <sup>#</sup>Integrated Cardio Metabolic Centre (ICMC), Karolinska Institutet, SE-141 57, Huddinge, Sweden

### Abstract

Taxanes are chemotherapeutic agents used in the treatment of solid tumors, particularly of breast, ovarian, and lung origin. However, patients show divergent therapy responses, and the molecular determinants of taxane sensitivity have remained elusive. Especially the signaling pathways that promote death of the taxane-treated cells are poorly characterized. Here we describe a novel part of a signaling route in which c-Myc enhances paclitaxel sensitivity through upregulation of miR-203b-3p and miR-203a-3p; two clustered antiapoptosis protein Bcl-xL controlling microRNAs. *In vitro*, the miR-203b-3p decreases the expression of Bcl-xL by direct targeting of the gene's mRNA 3'UTR. Notably, overexpression of the miR-203b-3p changed the fate of paclitaxel-treated breast and ovarian cancer cells from mitotic slippage to cell death. In breast tumors, high expression of the miR-203b-3p and *MYC* was associated with better therapy response and patient survival. Interestingly, in the breast tumors, *MYC* expression correlated negatively with *BCL2L1* expression but positively with miR-203b-3p and miR-203a-3p. Finally, silencing of *MYC* suppressed the transcription of both miRNAs in breast tumor cells. Pending further validation, these results may assist in patient stratification for taxane therapy.

*Translational Oncology* (2019) 12, 170–179

### Introduction

Taxanes are chemotherapeutic agents that disturb microtubule dependent processes, such as cell division, by altering microtubule dynamics. These drugs are widely used in the treatment of ovarian, breast, and lung cancer [1–3]. Taxanes, such as paclitaxel, have proved to be effective in the clinical setting, but like many other chemotherapy compounds, they are nonspecific cytotoxins that affect all cells in the body. Also, the molecular determinants of paclitaxel sensitivity in tumor cells have remained elusive [4]. Together, these characteristics result in adverse effects and variable treatment outcomes for the patients. For example, up to 70% of patients with high-grade ovarian tumors treated with a platinum-taxane combination relapse in a median of 15 months despite their initial treatment response [3]. Thus, there is a need for biomarkers

that could help to predict the sensitivity of tumors to paclitaxel therapy.

When high concentrations of paclitaxel are applied on cultured cancer cells, the mitotic spindle assembly is disrupted, which activates

Address all correspondence to: Marko J. Kallio, Institute of Biomedicine, Research Centre for Integrative Physiology and Pharmacology, University of Turku, Kiinamylynkatu 10, 20520 Turku, Finland. E-mail: [marko.kallio@utu.fi](mailto:marko.kallio@utu.fi)

<sup>1</sup>Conflicts of Interest: The authors declare no conflicts of interest.

Received 25 September 2018; Revised 1 October 2018; Accepted 1 October 2018

© 2018 The Authors. Published by Elsevier Inc. on behalf of Neoplasia Press, Inc. This is an open access article under the CC BY-NC-ND license (<http://creativecommons.org/licenses/by-nc-nd/4.0/>).

1936-5233/19

<https://doi.org/10.1016/j.tranon.2018.10.001>

the spindle assembly checkpoint causing a mitotic arrest [5,6]. The cells either die at the mitotic block or return to interphase without cell division, an event referred to as “exit” or “slippage”. Cells that abnormally exit mitosis can undergo post-mitotic death (PMD), arrest in interphase or G<sub>0</sub>, or continue cycling [7,8]. A competition between the cyclin B–dependent mitotic exit network and the increasing proapoptosis signaling determines a cancer cell's response to paclitaxel treatment. The mitotic exit network is a well-established cascade, but much less is known about the regulation of cell death during mitotic arrest and after slippage [8]. The PMD has potential clinical relevance since intratumoral paclitaxel concentrations may not be high enough to adequately activate the spindle assembly checkpoint in tumor cells but can instead allow slippage from mitosis accompanied with chromosome mis-segregation [9].

The intrinsic mitochondrial apoptosis pathway, consisting of effector proteins as well as pro- and antiapoptotic regulator proteins [10], has been suggested to be the main mediator of paclitaxel-induced death [11,12]. In addition to the master regulator of this cell death pathway, c-Myc (*MYC*) [12,13], the antiapoptotic Bcl-2 family member Bcl-xL (*BCL2L1*) is conceivably one of the key determinants of taxane sensitivity in cancer cell and xenograft models [14–16]. High Bcl-xL expression has indeed been associated with paclitaxel resistance in solid tumors [17,18]. However, not much is known about the regulation of Bcl-xL expression and activity. Topham and coworkers [12], Eischen et al. [19], and Maclean et al. [20] have proven that c-Myc suppresses Bcl-xL expression, but the molecular mechanism remains unclear.

MicroRNAs (miRNA) belong to the family of small regulatory RNAs, and they control the expression of most human genes at post-transcriptional level [21]. miRNAs may also possess diagnostic value as tumor biomarkers [22]. In this study, we aimed to identify novel *BCL2L1* regulating miRNA(s) whose altered expression would modulate cancer cells' survival after paclitaxel treatment *in vitro* and *in vivo*. We present the first evidence that miR-203b-3p and miR-203a-3p are among the c-Myc–regulated elements that control the expression of Bcl-xL and thereby influence tumor cells' sensitivity to paclitaxel therapy.

## Materials and Methods

### Cell Culture

293T, MDA-MB-231 SA (Theresa A. Guise, University of Virginia, Charlottesville, VA), OVCAR-8 (DCTD Tumor/Cell Line Repository, NCI), and CaOV-3 (ATCC) cells were cultured in DMEM/F12 (Sigma-Aldrich, St. Louis, MO) supplemented with 10% inactivated fetal bovine serum (FBS), 1 mM L-glutamine, and 1% penicillin-streptomycin, as well as 0.1 mM nonessential amino acids for MDA-MB-231 and sodium pyruvate (1 mM) for CaOV-3. MCF-7 (ICLC HTL95021) cells were grown in DMEM (1000 mg/l glucose, Sigma-Aldrich) supplemented with FBS, 2 mM L-glutamine, and penicillin-streptomycin. The MDA-MB-231 SA cells are bone metastatic and were spontaneously derived from the parental cells during a long *in vitro* culture [23].

### Transient Transfection of miRNAs and siRNAs

miRIDIAN miRNA mimics and the *MYC* siRNA were purchased from GE Dharmacon (Lafayette, CO) and used at a 50-nM concentration. HiPerFect transfection reagent (Qiagen, Valencia, CA) was used to transiently transfect cells with miRNA mimics and siRNAs, and Lipofectamine 3000 (Invitrogen, Thermo Fisher

Scientific, Waltham, MA) was used for co-transfecting oligonucleotides and plasmids.

### Live-Cell Imaging

To study the effect of miRNAs on paclitaxel sensitivity, we transfected the cells with miRNA mimics, and 28 to 29 hours later, added 10 nM paclitaxel (Sigma-Aldrich) to the culture medium. Imaging with Incucyte live-cell imaging device (Essen Instruments Ltd. Hertfordshire, UK) was started immediately after the drug was supplemented, and the filming continued for 48 to 72 hours at a 30-minute image capture interval. The cell fates profiles were determined with visual inspection of the phase-contrast image sequences [8,12,24]. Briefly, death in mitosis (DiM) was determined as death during the drug-induced mitotic arrest based on morphological changes; rounded mitotic cells started surface blebbing, shrank, and disaggregated. PMD was determined as death of a post-mitotic interphase (flat) cell in G<sub>1</sub>, S, or G<sub>2</sub> phase; cells that had exited prolonged mitotic arrest (changed from a round cell morphology to a flat morphology) started intense surface blebbing, shrank, and often disaggregated into a number of membrane-bound particles.

### CellTiter-Glo and Luciferase Reporter Assays

Cell viability was measured with the CellTiter-Glo Luminescent Assay (Promega, Madison, WI) and EnSight Multimode Plate Reader (PerkinElmer, Waltham, MA) according to the manufacturer's instructions. The luciferase reporter assays were performed in MDA-MB-231 SA or 293T cells according to the previously described procedure [25]. The *MIR203A*-pGL3 construct contained bp 13 to 1183 upstream of *MIR203A*, as described before [26].

### RNA Isolation and miRNA qPCR

For quantitative miRNA PCR, samples were collected 72 hours after transfection and the paclitaxel-treated samples after an overnight drug treatment. The relative expression of mature miRNAs was measured as described previously [25].

### Immunoblotting

Cells were lysed for immunoblotting either with APC buffer as previously described [27] or with RIPA buffer (50 mM Tris-HCl pH 7.5, 150 mM NaCl, 0.5% DOC, 0.1% SDS, 1% NP-40), supplemented with phosphatase and protease inhibitors, and sonication. Membranes were blocked with 5% milk/TBS-T (0.1% Tween) before primary antibody incubations. The primary antibodies included rabbit anti-Bcl-xL (1:1000; #2764 Cell Signaling Technology, Danvers, MA), rabbit anti-c-Myc (Y69; 1:1000; ab32072 Abcam, Cambridge, UK), mouse anti-cleaved PARP (Asp214; 1:1000; #9546 Cell Signaling Technology), rabbit anti-cleaved caspase 3 (Asp175; 1:1000; #9664 Cell Signaling Technology), and mouse anti-GAPDH (1:30000, HyTest Ltd., Turku, Finland). HRP-linked secondary antibodies were used at 1:5000 concentration, and protein signals were detected with chemiluminescence.

### Clinical Data Analysis

**TCGA Cohorts.** The TCGA repository was used to study patient survival and miRNA expression (level 3), obtained with Illumina sequencing [28], in 1172 breast cancer cases. The information regarding The Cancer Genome Atlas (TCGA) ovarian cancer cohort data has been previously described [29].

**Bergen Cohort.** The cohort has been described in detail previously [30,31]. For description of the sample collection,

miRNA profiling, and data analysis, please refer to [29] with the following refinements: demultiplexing was performed with the Illumina CASAVA software, sequence quality was analyzed with FastQC, and samples with less than 300,000 reads were excluded, as well as miRNAs with less than 20 sequencing reads in 25% or more of the samples. In total, the miRNA profiling included 466 mature human miRNAs in 200 patients. miRNA read counts were transformed and normalized using the rlog function of the DeSeq2 R package [32]. From the same tumor samples, the mRNA levels were assayed using the Illumina HT-12 cDNA microarray platform. Raw intensities were processed by quantile normalization based on a set of high-quality probes, and batch correction was performed to adjust for differences between runs [33,34]. Data from cDNA microarray and miRNA sequencing were available from 190 patients (epirubicin;  $n = 85$ , paclitaxel;  $n = 105$ ).

### Statistical Analysis

Paired, two-tailed Student's  $t$  test was used to perform statistical analyses for the *in vitro* assays. For comparing differences in gene and miRNA expression between two or more groups in the cohort datasets,  $t$  test and ANOVA were applied, respectively. For assessment of associations between survival times and single categorical variables, log-rank tests were performed. Statistical significance was defined as  $P \leq .05$  (\*),  $P \leq .01$  (\*\*), and  $P \leq .001$  (\*\*\*). Values are presented as the average  $\pm$  standard deviation (S.D.).

## Results

### miR-203b-3p-induced Modulation of Cell Fate upon Paclitaxel Treatment

To identify novel miRNAs that cause a change in the cell fate upon paclitaxel treatment, we searched for potential candidates among the top 50 miRNAs that are predicted to target *BCL2L1* (Table S1): a component of the mitochondrial apoptosis pathway [10] and a key regulator of taxane-induced cancer cell death [12,14–16,24]. Among these candidates, we found four miRNAs (miR-342-3p, miR-203b-3p, miR-505-5p, miR-361-3p) that potentially regulate Bcl-xL and paclitaxel sensitivity in cancer cells. These miRNAs were noted to negatively correlate with *BCL2L1* levels and positively associate with taxane response in the NCI cell line database (Table S2). Moreover, low expression of these four miRNAs correlated with reduced patient survival in at least one of the three studied breast and ovarian cancer cohorts (Figure S1). The steps of the candidate miRNA filtering are presented in more detail in Supplementary Figure 1.

Next, the four candidate miRNAs were applied in live-cell imaging analysis where the fate of miRNA mimic transfected MDA-MB-231 SA breast cancer cells and OVCAR-8 and CaOV-3 ovarian cancer cells was determined upon treatment with clinically relevant paclitaxel dose (10 nM) [9]. Out of the tested four miRNAs, only miR-203b-3p considerably elevated the rate of cell DiM in all cell lines (Figure 1, A–B,

Figure S2); in average by 17.3% ( $\pm 3.5\%$ ,  $P = .01$ ), 14.0% ( $\pm 6.9\%$ ), and 15.3% ( $\pm 5.3\%$ ,  $P = .05$ ) in MDA-MB-231 SA, OVCAR-8, and CaOV-3, respectively. The miR-203b-3p was also confirmed to elevate DiM to a similar extent in the hormone receptor–positive breast cancer cell line MCF-7, in average by 8.7% ( $\pm 4.2\%$ ,  $P = .04$ ; Figure 1, A–B). The intrinsic rate of DiM varied between the cell lines, with the highest frequency in OVCAR-8. However, this did not correlate with the cell death promoting potency of the miR-203b-3p. Death after slippage (PMD) was significantly increased by excess miR-203b-3p only in the breast cancer cell lines, in average by 14.0% ( $\pm 5.0\%$ ,  $P = .03$ ) in MDA-MB-231 and by 12.0% in MCF-7 ( $\pm 9.2\%$ ,  $P = .01$ ) (Figure 1, A–B). The inherent PMD frequency was lower in the breast cancer cell lines compared to the ovarian cancer cell lines, which may partially explain the observed difference in the miR-203b-3p effect. In MDA-MB-231 SA cells, miR-203b-3p also advanced the timing of DiM and PMD, in average by 3.3 hours ( $\pm 0.7$  hour) and 2.6 hours ( $\pm 1.8$  hours,  $P = .03$ ), respectively (Figure 1, C–D). The onset of DiM was intrinsically slowest in the MDA-MB-231 SA cells, but on the other hand, miR-203b-3p did not accelerate PMD in CaOV-3 cells, although the timing of PMD was longest in these ovarian cancer cells (Figure 1, C–D).

In conclusion, excess of miR-203b-3p alters the cell fate upon paclitaxel treatment; the breast and ovarian cancer cells die in M-phase at a higher rate rather than slipping out from mitosis, and a higher fraction of the slipped cells undergo PMD.

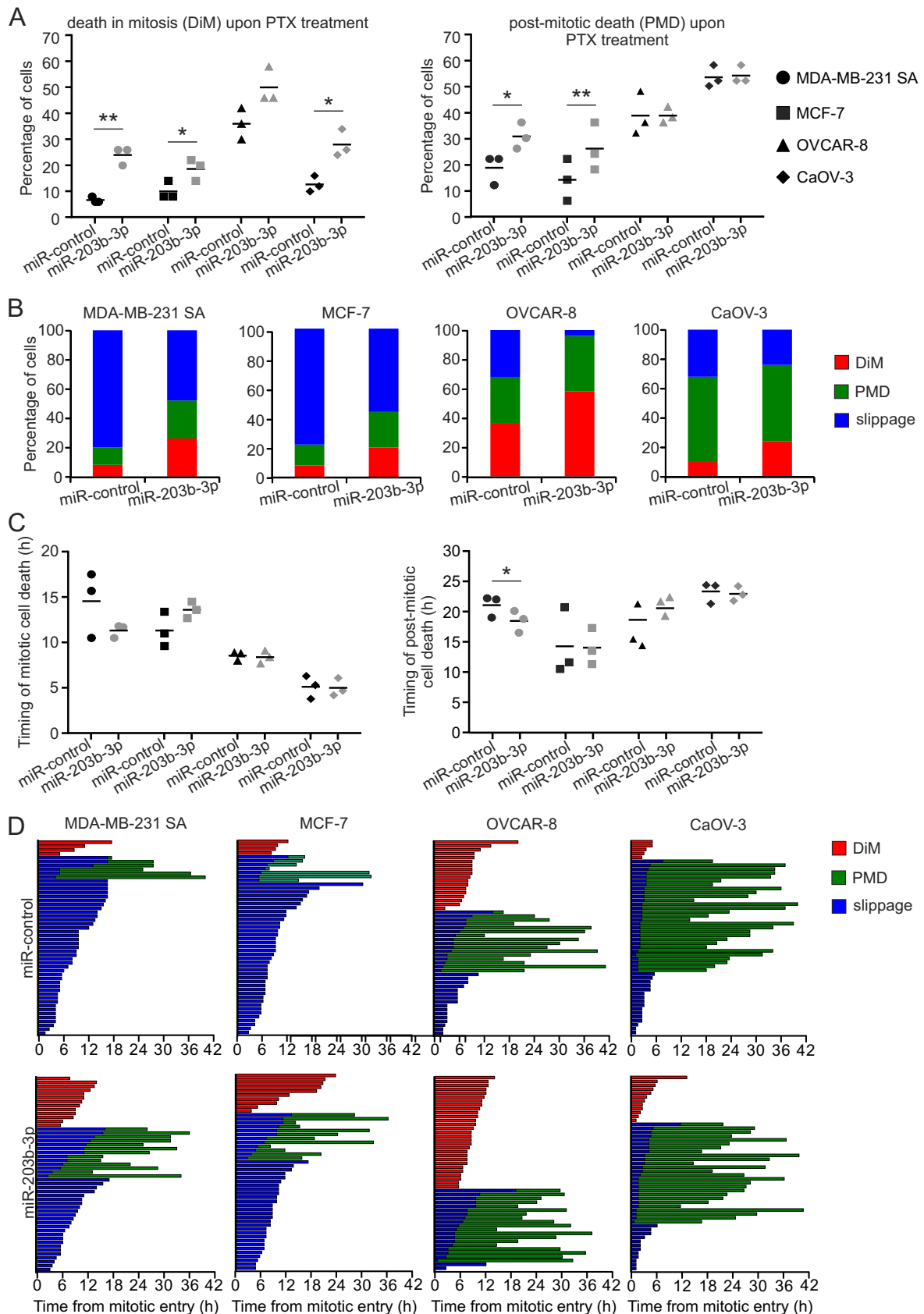
### Improved Cancer Cell Death and Patient Treatment Response by High Levels of miR-203b-3p

In the further phenotypic studies, we focused on the representative breast and ovarian cancer cell lines MDA-MB-231 SA and CaOV-3, as the miR-203b-3p effect on paclitaxel-induced cell death, especially DiM, was most notable in these cells. First, to strengthen our findings from live-cell imaging assays, we assessed cell viability and the expression levels of cell death markers at cell population scale in miR-203b-3p overexpressing MDA-MB-231 SA and CaOV-3 cell lines after 48-hour paclitaxel treatment. Indeed, the expression of cleaved PARP and cleaved caspase 3 proteins was increased 1.3- to 3.3-fold in the miR-203b-3p overexpressing cell populations compared to the controls (Figure 2A), suggesting an increase of caspase-mediated cell death. Moreover, Cell-Titer Glo assay indicated significant decreases in average cell viability in MDA-MB-231 SA (34.4  $\pm 5.6\%$ ,  $P = .009$ ) and CaOV-3 cells (23.0  $\pm 6.5\%$ ,  $P = .03$ ) after miR-203b-3p transfections compared to miR-control transfected cell populations (Figure 2B). Furthermore, live-cell imaging demonstrated a decline in the proliferation curvatures of paclitaxel treated MDA-MB-231 SA and CaOV-3 cells with excess of miR-203b-3p in comparison to controls (Figure S3, C–D). Importantly, no significant difference in growth or cell viability was observed between miR-control and miR-203b-3p overexpressing cell populations in unperturbed culture conditions over the course of 3 days after miRNA transfection (Figure S3, A–B).

**Figure 1.** Excess miR-203b-3p alters the fate of breast and ovarian cancer cells cultured in the presence of paclitaxel (PTX). (A) The graphs show the percentage of cells undergoing DiM or PMD in the miR-control (black) and miR-203b-3p (gray) overexpressing cell populations treated with 10 nM PTX for 48 hours. Each dot represents the average of an experiment, and the line indicates the mean from three experiments ( $n = 150$  cells). (B) The bar graphs demonstrate the proportion of each cell fate (DiM = red, PMD = green, slippage = blue) in representative experiments from A. (C) The timing of DiM and PMD in cell populations presented in panel A. (D) Line graphs showing the cell fate and duration of PTX-induced mitotic arrest for individual cells in miR-control and miR-203b-3p transfected cell populations from representative experiments (DiM = red, PMD = green, slippage = blue). Time “0” represents the mitotic entry.

Since high expression of miR-203b-3p promotes DiM instead of mitotic slippage *in vitro* in breast and ovarian carcinoma cells treated with clinically relevant paclitaxel concentration [9], we speculated that the

same may also occur in tumor cells. To get insights into this notion, we retrospectively analyzed patient survival in relation to miR-203b-3p expression in a TCGA breast cancer dataset ( $n = 1172$ ). The results



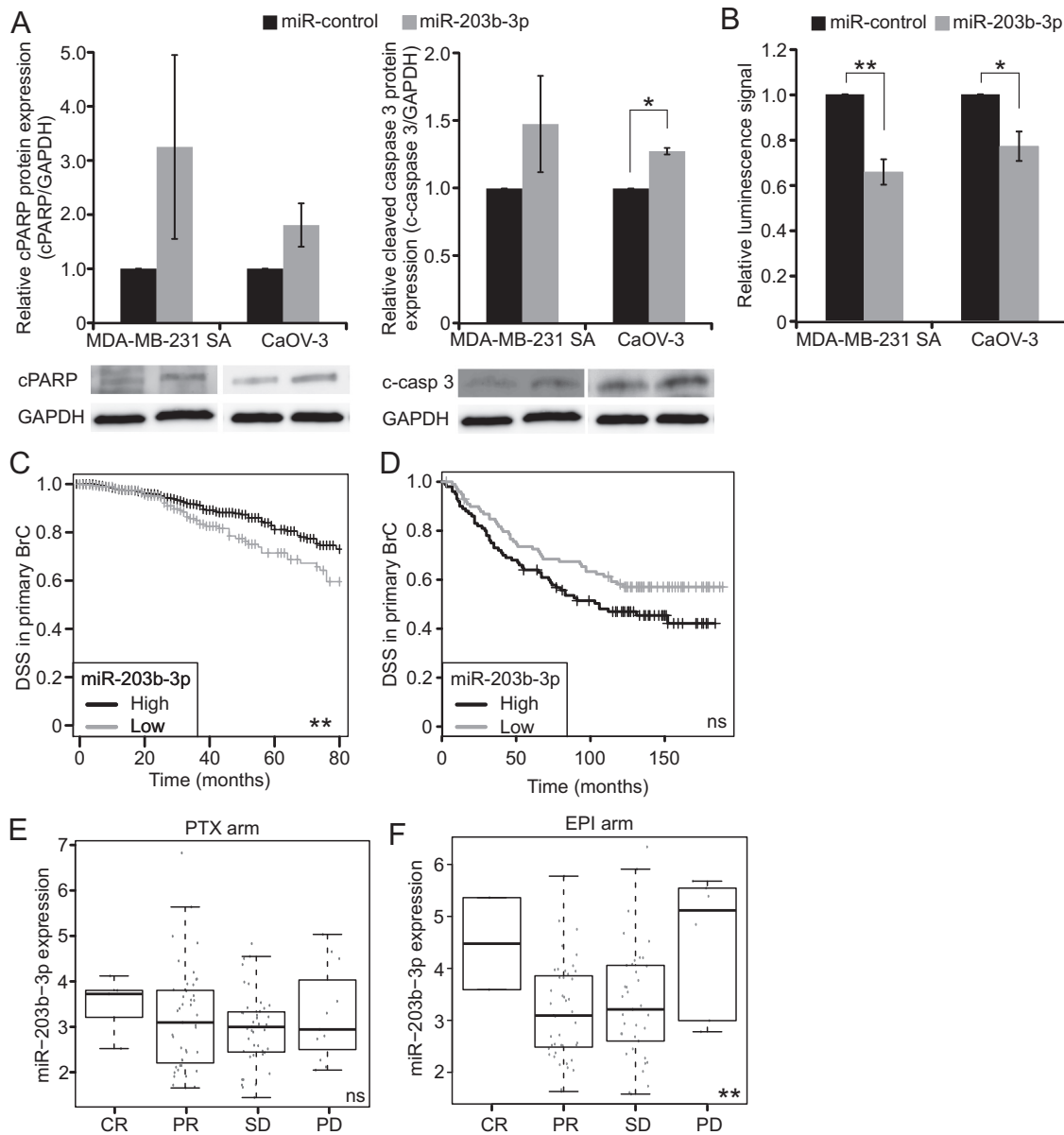


**Figure 2.** High levels of miR-203b-3p promote PTX-induced cell death and treatment response. (A) The levels of cleaved PARP and cleaved caspase 3 proteins in the indicated cell lines overexpressing miR-203b-3p or miR-control, assessed 48 hours after addition of 10 nM PTX. Images of representative immunoblots are shown below. (B) Measurement of cell viability with Cell-Titer Glo in the same experimental setup. Data are from two to three independent experiments, shown as mean  $\pm$  S.D. (C) Kaplan-Meier plots representing disease-specific survival (DSS) of breast cancer patients from the TCGA breast ( $n = 1172$ ) and (D) Bergen cohort ( $n = 190$ ), divided into groups with low and high miR-203b-3p expression. (E-F) miR-203b-3p expression in the different therapy response groups among breast cancer patients in the PTX ( $n = 105$ ) and EPI ( $n = 85$ ) therapy arms of the Bergen cohort. Each dot depicts an individual tumor/patient. The boxes span the interquartile range, with whiskers extending to 1.5 times the range from the median to the bounds of the box, or the most extreme observation if this is within the normal range of the whiskers. CR = complete response, PR = partial response, SD = stable disease, PD = progressive disease.

show a small but significant difference linking improved disease-specific patient survival with high miR-203b-3p levels ( $P = .008$ , Figure 2C). We did not find similar association between the miR-203b-3p expression and patient survival in a smaller breast cancer cohort (Bergen, Figure 2D, for PTX and EPI arms Figure S4, A-B). However, in the Bergen cohort, where the patients were randomized to paclitaxel or epirubicin therapy, we did observe a slightly higher miR-203b-3p expression in patient groups that had responded well to paclitaxel therapy (Figure 2E and Figure S4C). In the epirubicin group, miR-203b-3p expression did not show a similar pattern. On the contrary, the mean

miR-203b-3p level was highest in the patients with poorest response to epirubicin and, thus, progressive disease ( $P = .01$ , Figure 2F and S4D).

#### Direct Suppression of the Antiapoptotic *BCL2L1*

To test if the miR-203b-3p binds to its predicted target gene *BCL2L1*, we utilized the luciferase reporter assay. Excess of miR-203b-3p significantly suppressed the luciferase activity produced by a *BCL2L1* 3'UTR-luciferase construct when compared to miR-control ( $0.78 \pm 0.13$ ,  $P = .04$ , Figure 3B). Importantly, the binding of miR-203b-3p to *BCL2L1* led to a slight but consistent decrease in

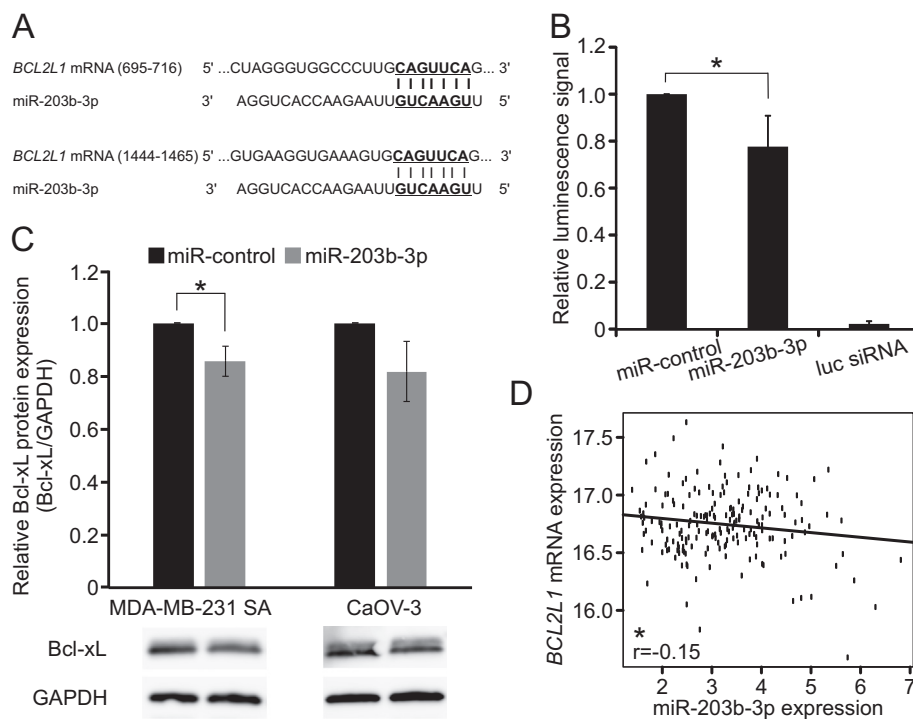


**Figure 3.** miR-203b-3p binds directly to the *BCL2L1* 3'UTR and lowers the protein levels. (A) A schematic representation of the two predicted miR-203b-3p binding sites in the *BCL2L1* 3'UTR and (B) quantification of relative luciferase activity in MDA-MB-231 SA cells 48 hours after transfection of *BCL2L1* 3'UTR-luciferase plasmid and miR-control, miR-203b-3p, or luciferase siRNA (positive control). (C) A bar graph with quantification of relative Bcl-xL protein levels in the indicated cells lines 48 hours after transfection with miR-control or miR-203b-3p. Bcl-xL expression was normalized to GAPDH, and representative immunoblots are shown below. All data are from three to four independent experiments. (D) A scatter plot with regression line and Pearson correlation ( $r$ ) from the Bergen breast cancer cohort for *BCL2L1* and miR-203b-3p.  $N = 190$ .

Bcl-xL protein levels of MDA-MB-231 SA ( $14.4 \pm 5.7\%$ ,  $P = .05$ ) and CaOV-3 ( $18.3 \pm 11.3\%$ ) cells (Figure 3C). Supporting the results from cultured cancer cells, miR-203b-3p and *BCL2L1* exhibited a modest but significant negative correlation in the breast tumors from the Bergen cohort ( $-0.15$ ,  $P = .04$ , Figure 3D). The data support our notion that miR-203b-3p may enhance cell death upon paclitaxel treatment by contributing to the suppression of the antiapoptotic Bcl-xL via direct association with the *BCL2L1* 3'UTR region.

#### Association of MYC with Bcl-xL, miR-203b-3p, and miR-203a-3p in Breast Tumors

Several groups have demonstrated a negative regulation of Bcl-xL by the oncogene *c-Myc*, both with *in vitro* and *in vivo* models [12,19,20]. Here, we retrospectively studied the association of these two genes and miR-203b-3p in the Bergen breast cancer cohort. In line with the previous studies, patients with high *MYC* expression had significantly lower *BCL2L1* levels ( $P = .02$ , Figure S5A); *MYC* and *BCL2L1* also exhibited a direct negative correlation in the breast tumors ( $-0.26$ ,  $P < .001$ , Table S3) that arose almost solely from the paclitaxel arm samples ( $-0.46$ ,  $P < .001$ ; Figure 4A).

Another interesting finding from the breast tumors was the positive correlation of *MYC* and miR-203b-3p (Table S3), especially in the paclitaxel therapy group ( $0.15$ , Figure 4B). *c-Myc* is known to control the expression of several miRNAs [35], suggesting a possible transcriptional induction of miR-203b-3p by *c-Myc* in the breast tumors. Moreover, we observed a similar positive correlation ( $0.17$ , Figure 4C) in the paclitaxel therapy group between *MYC* and miR-

203a-3p, which resides in a genomic cluster with the miR-203b. Also the distinct intercorrelation of miR-203b-3p and miR-203a-3p levels in the breast tumors ( $0.69$ ,  $P < .001$ , Figure 4D) strongly implies that these clustered miRNAs share a transcriptional regulator(s). Since miR-203a-3p has also been reported to suppress Bcl-xL expression [36], yet indirectly, these findings raise a possibility that both miR-203a and miR-203b act as links in the *c-Myc*/Bcl-xL regulatory axis, the activity of which is associated with the efficacy of paclitaxel treatment.

#### Regulation of Paclitaxel Sensitivity by *c-Myc*, Potentially via miR-203s and Bcl-xL

To have molecular-level evidence for support of our findings in breast tumors, we explored the *c-Myc*/miR-203/Bcl-xL-axis in cultured cancer cell models. First, the positive correlation of *MYC* with miR-203a-3p and miR-203b-3p *in vivo* prompted us to measure the expression of the mature miRNAs in *c-Myc* depleted cells CaOV-3 cells (Figure S5B), which exhibit the highest endogenous levels of these miRNAs among the cell lines used in this study. The results indicated remarkable decreases of miR-203a-3p and miR-203b-3p levels upon *MYC* silencing and culture in the presence of 10 nM paclitaxel ( $39.2\% \pm 29.7\%$  and  $65.3\% \pm 20.2\%$ ,  $P = .03$ , respectively) (Figure 5A and Figure S5C). This result is in line with the positive *MYC*-miRNA correlations observed *in vivo*. Supporting the hypothesis that *c-Myc* regulates *MIR203* expression via transcription, *c-Myc* CHIP data from the ENCODE project [37] demonstrated an enrichment of *c-Myc* instantly upstream of the *MIR203* locus (Figure 5B). This genomic site was also

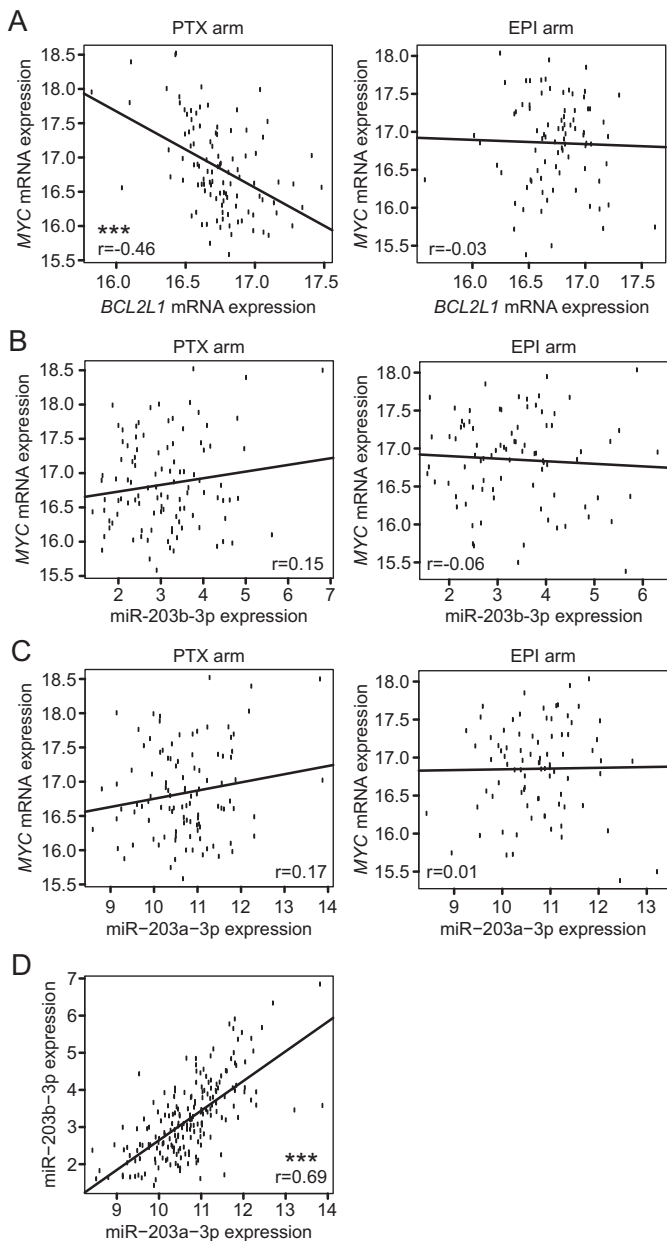


**Figure 4.** c-Myc/miR-203/Bcl-xL-axis in breast cancer *in vivo*. (A-D) Scatter plots with regression lines and Pearson correlations ( $r$ ) from the Bergen breast cancer cohort data for (A) *MYC* and *BCL2L1* (PTX,  $P < .001$ ), (B) *MYC* and miR-203b-3p, (C) *MYC* and miR-203a-3p, and (D) miR-203b-3p and miR-203a-3p ( $P < .001$ ). In panels A-C, separate plots from paclitaxel (PTX,  $n = 105$ ) and epirubicin (EPI,  $n = 85$ ) therapy groups are presented; data in panel D are from the whole cohort ( $n = 200$ ).

positive for H3K4me histone modification: a marker for active promoters. As an experimental proof that c-Myc regulates *MIR203* transcription, the activity of the *MIR203* promoter (Figure 5B) was diminished by 55.1% ( $\pm 2.9\%$ ,  $P = .001$ ) in c-Myc silenced cells in comparison to controls (Figure 5C).

Finally, we confirmed the finding of Topham et al. [12] that a high *MYC* expression is a favorable prognostic factor for the survival of breast cancer patients, in a larger dataset (Figure S5D). Moreover, the patient treatment annotations in the analyzed cohort revealed that *MYC* levels are associated with the patient survival only upon paclitaxel treatment but not in the epirubicin-treated patients (Figure 5, D-E).

## Discussion

The molecular determinants of tumor cells' response to taxanes have remained poorly understood [4]. Here, we show for the first time that excess miR-203b-3p promotes cell death instead of mitotic slippage in breast and ovarian cancer cells cultured in the presence of a low, clinically relevant paclitaxel dose. Moreover, high levels of miR-203b-3p associate with better survival of breast cancer patients. The sensitization to paclitaxel by miR-203b-3p is, at least partially, achieved through direct suppression of the antiapoptotic Bcl-xL protein. Thus, these novel findings reinforce the previous perceptions about the importance of Bcl-xL in the regulation of paclitaxel sensitivity [14–18] and demonstrate the potential of specific miRNAs as predictors of drug response in cancer patients.

c-Myc is often deregulated in tumors and has a peculiar dual role in cancer: it induces cell proliferation but on the other hand also promotes apoptosis by controlling the mitochondrial apoptosis pathway [12,13,38]. According to its proapoptotic function, high c-Myc levels have been shown to sensitize cultured cancer cells to anti-mitotic cancer therapeutics and associate with better treatment response in breast cancer patients [12]. We also observed a significant correlation between high *MYC* expression and superior survival of paclitaxel-treated breast cancer patients. The lack of this correlation in the epirubicin therapy arm indirectly implies that c-Myc may serve as a prognostic factor specifically for anti-mitotic cancer therapeutics. Moreover, our findings propose a novel mechanism (Figure 6) for the c-Myc-mediated sensitization to paclitaxel, which may, at least partially, depend on the transcriptional induction of two Bcl-xL regulating miRNAs, miR-203b-3p and miR-203a-3p [36].

Specific miRNAs, such as miR-203b-3p and miR-203a-3p, can be contributing factors in the previously unidentified link between c-Myc and Bcl-xL, as is supported by the following notions. First, the reported suppression of both mRNA and protein levels of Bcl-xL by c-Myc suggests regulation at the transcriptional level, while the requirement for active protein synthesis proposes that the mechanism is indirect [19,20]. Indeed, miRNAs can regulate the expression of their target genes by both degrading the target gene mRNA and/or inhibiting its translation into protein [21]. Here, we demonstrate for the first time that miR-203b-3p suppresses Bcl-xL protein expression *via* direct binding to the gene's mRNA 3'UTR and correlates negatively with *BCL2L1* mRNA expression in breast tumors. Secondly, several miRNAs are transcriptionally regulated by c-Myc [35]. In the breast cancer cohort, the levels of two adjacent miRNAs, the miR-203b-3p and miR-203a-3p, which has been reported to indirectly repress Bcl-xL protein levels [36], correlated positively with *MYC* expression. Moreover, the significant declines in the activity of the *MIR203A/B* promoter and in the levels of both miRNAs in c-Myc depleted cells, along with the ENCODE ChIP data showing c-Myc enrichment at the *MIR203A/B* promoter, support the concept of c-Myc-induced transcription of these miRNAs. The induction of several Bcl-xL suppressing miRNAs, including miR-203b-3p and miR-203a-3p, provides one feasible solution for the yet unidentified mechanism of c-Myc-mediated Bcl-xL suppression.

Interestingly, the let-7 miRNA family was recently reported to be upregulated in a c-Myc-driven manner in breast, lung, and hematopoietic cancers upon treatment with histone deacetylase inhibitors (HDACi) [39,40]. This led to the suppression of Bcl-xL, a let-7 target gene, which was essential for the drug-induced cell death in this context [39,40]. How widespread the mechanism of c-Myc-mediated suppression of Bcl-xL by specific miRNAs is and which drug treatments trigger the signaling event merit further studies. Our



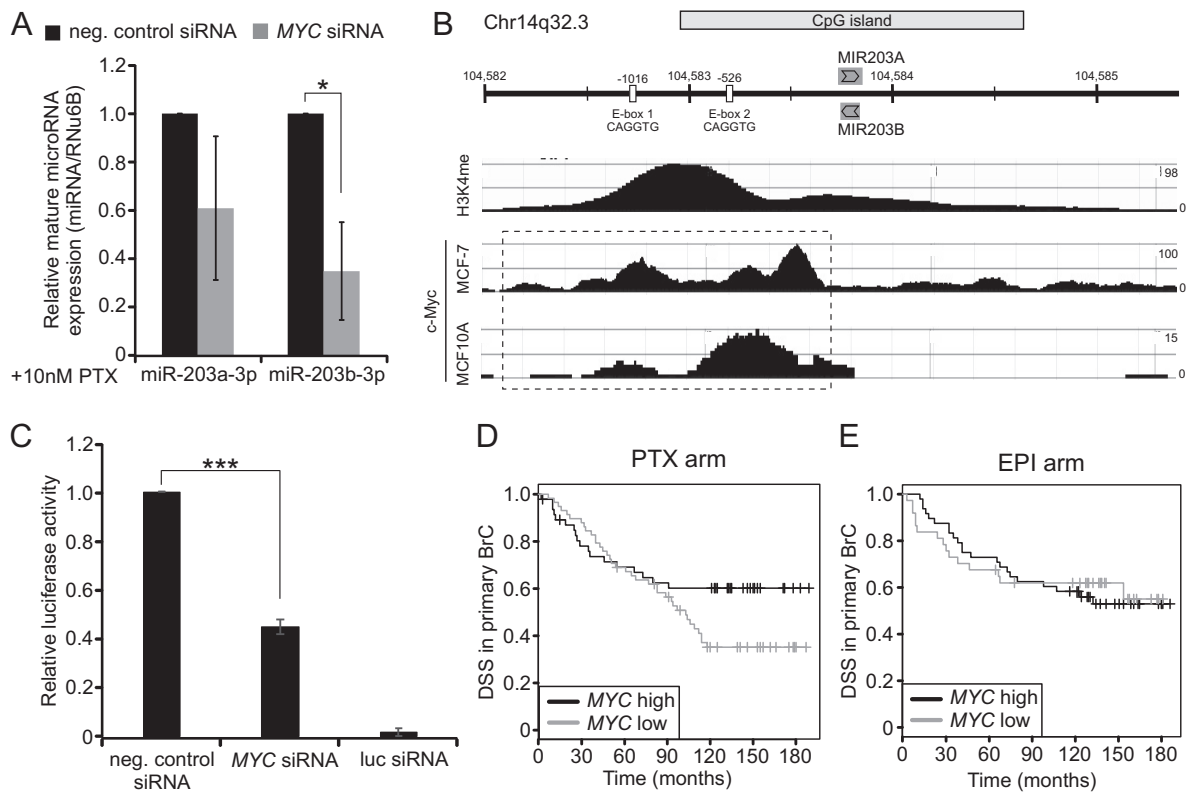


**Figure 5.** c-Myc controls the expression of Bcl-xL regulating miRNAs and enhances patient survival upon paclitaxel treatment. (A) Quantification of relative mature miR-203a-3p and miR-203b-3p levels in CaOV-3 cells 72 h after MYC siRNA transfection in comparison to control. Cells were treated overnight with 10 nM paclitaxel before harvesting the samples. The data are from 4 independent experiments. (B) The genomic locus of *MIR203A* and *MIR203B* on chr14q32.3. The promoter sequence, spanning ~1.2 kb upstream of the miRNA genes, harbors two conserved E-box sequences. Below are presented H3K4me and c-Myc ChIP data from the ENCODE database [35], indicating enrichment of these markers/proteins upstream of the *MIR203A/B* locus, in breast cancer cells lines MCF-7 and MCF10A. The IDs for the datasets presented here are GSM1586404, GSM822301, and GSM935441. (C) Co-transfection of MYC siRNA diminishes the activity of *MIR203* WT promoter compared to co-transfection of negative control siRNA. Luciferase siRNA served as a positive control, and data are from three experiments. (D-E) Kaplan-Meier plots representing disease-specific survival of breast cancer patients from the Bergen cohort with high and low MYC expression, treated with (D) paclitaxel (PTX,  $n = 105$ ) or (E) epirubicin (EPI,  $n = 85$ ).

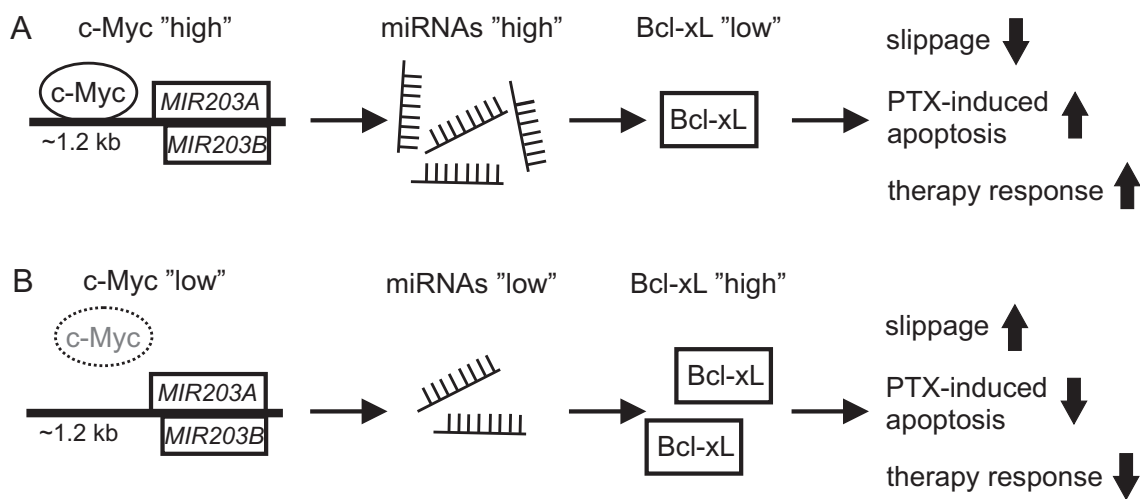


**Figure 6.** A schematic model of how the c-Myc/miR-203/Bcl-xL-axis may influence the paclitaxel sensitivity of tumor cells. According to our results, we present a model where (A) high c-Myc levels lead to increased expression of the clustered Bcl-xL regulating miRNAs, miR-203a-3p, and miR-203b-3p. The elevated levels of these miRNAs lead to suppression of Bcl-xL expression, increased cell death, and decreased slippage upon paclitaxel treatment and, thus, improved therapy outcome. On the other hand, (B) low c-Myc levels may be associated with poorer paclitaxel therapy response due to the lower levels of the Bcl-xL regulating miRNAs, higher expression of the antiapoptotic Bcl-xL, and the consequent increased frequency of slippage from paclitaxel-mediated mitotic block.

results from *in vivo* and *in vitro* studies suggest that paclitaxel treatment may modulate the activity of the c-Myc/miR203/Bcl-xL axis. Paclitaxel and HDACi-induced changes in the chromatin condensation can be a contributing factor in the drug-induced switch of c-Myc transcriptional activity. Intriguingly, at therapeutic concentrations, both drugs can induce a similar mitotic phenotype: a transient mitotic arrest followed by slippage [9,41,42], which as an event may cause changes in the c-Myc transcription factor function.

This study sheds new light on the molecular mechanism of c-Myc-mediated sensitization to taxane therapy by providing preliminary evidence for existence of a c-Myc/miR-203/Bcl-xL pathway that contributes to the modulation of cancer cells' response to paclitaxel treatment *in vitro* and *in vivo*. Moreover, our results imply that especially *MYC* but potentially also the specific Bcl-xL regulating miRNAs, such as miR-203b-3p, may be harnessed as predictors of tumor cells' drug sensitivity in future. Finally, the data presented here also support the promising concept of combining inhibitors of the Bcl-2 family proteins with taxanes to improve the treatment response, which has already yielded promising results in preclinical models [14,18,43,44].

### Acknowledgements

The authors thank Dr. Olli Carpen (University of Turku and Turku University Hospital) and Dr. Theresa Guise for providing cell lines used in this study. Dr. Christophe Denoyelle (Université de Caen Normandie, France) is thanked for providing the *BCL2L1* 3'UTR-luciferase plasmid and Prof. Thomas Brabletz (FAU University Erlangen-Nürnberg, Germany) for sharing the *MIR203* promoter-pGL3 constructs. The authors wish to thank Prof. Jukka Westermark (Turku Centre for Biotechnology) for providing the *MYC* siRNA. This study was supported by an Academy of Finland grant (268360). S. A. received funding from the Turku Doctoral Programme of Molecular Medicine, the Finnish Cultural Foundation and, and M. J. K. from the Finnish Cancer Institute.

### Appendix A. Supplementary data

Supplementary data to this article can be found online at <https://doi.org/10.1016/j.tranon.2018.10.001>.

### References

- Jordan MA and Wilson L (2004). Microtubules as a target for anticancer drugs. *Nat Rev Cancer* **4**, 253–265. <https://doi.org/10.1038/nr1317>.
- Fraci G, Comella P, Rinaldo M, Iodice G, Di Bonito M, D' Aiuto M, Petrillo A, Lastoria S, Siani C, and Comella G, et al (2009). Preoperative weekly cisplatin-epirubicin-paclitaxel with G-CSF support in triple-negative large operable breast cancer. *Ann Oncol* **20**, 1185–1192. <https://doi.org/10.1093/annonc/mdn748>.
- Vasey PA, Jayson GC, Gordon A, Gabra H, Coleman R, Atkinson R, Parkin D, Paul J, Hay A, and Kaye SB, et al (2004). Phase III randomized trial of docetaxel-carboplatin versus paclitaxel-carboplatin as first-line chemotherapy for ovarian carcinoma. *J Natl Cancer Inst* **96**, 1682–1691. <https://doi.org/10.1093/jnci/djh323>.
- Weaver BA (2014). How Taxol/paclitaxel kills cancer cells. *Mol Biol Cell* **25**, 2677–2681. <https://doi.org/10.1091/mbc.E14-04-0916>.
- Yvon A-MM, Wadsworth P, and Jordan MA (1999). Taxol suppresses dynamics of individual microtubules in living human tumor cells. *Mol Biol Cell* **10**, 947–959. <https://doi.org/10.1091/mbc.10.4.947>.
- Musacchio A and Salmon ED (2007). The spindle-assembly checkpoint in space and time. *Nat Rev Mol Cell Biol* **8**, 379–393. <https://doi.org/10.1038/nrm2163>.
- Brito DA and Rieder CL (2009). The ability to survive mitosis in the presence of microtubule poisons differs significantly between human nontransformed (RPE-1) and cancer (U2OS, HeLa) cells. *Cell Motil Cytoskeleton* **66**, 437–447. <https://doi.org/10.1002/cm.20316>.
- Gascoigne KE and Taylor SS (2008). Cancer cells display profound intra- and interline variation following prolonged exposure to antimetabolic drugs. *Cancer Cell* **14**, 111–122. <https://doi.org/10.1016/j.ccr.2008.07.002>.
- Zasadil LM, Andersen KA, Yeum D, Rocque GB, Wilke LG, Tevaarwerk AJ, Raines RT, Burkard ME, and Weaver BA (2014). Cytotoxicity of paclitaxel in breast cancer is due to chromosome missegregation on multipolar spindles. *Sci Transl Med* **6**. <https://doi.org/10.1126/scitranslmed.3007965> [229ra43-229ra43].
- Youle RJ and Strasser A (2008). The BCL-2 protein family: opposing activities that mediate cell death. *Nat Rev Mol Cell Biol* **9**, 47–59. <https://doi.org/10.1038/nrm2308>.
- Kutuk O and Letai A (2008). Alteration of the mitochondrial apoptotic pathway is key to acquired paclitaxel resistance and can be reversed by ABT-737. *Cancer Res* **68**, 7985–7994. <https://doi.org/10.1158/0008-5472.CAN-08-1418>.
- Topham C, Tighe A, Ly P, Sansom OJ, Cleveland DW, Correspondence SST, Bennett A, Sloss O, Nelson L, and Ridgway RA, et al (2015). MYC is a major determinant of mitotic cell fate. *Cancer Cell* **28**, 129–140. <https://doi.org/10.1016/j.ccell.2015.06.001>.
- Muthalagu N, Junttila MR, Wiese KE, Wolf E, Morton J, Bauer B, Evan GI, Eilers M, and Murphy DJ (2014). BIM is the primary mediator of MYC-induced apoptosis in multiple solid tissues. *Cell Rep* **8**, 1347–1353. <https://doi.org/10.1016/j.celrep.2014.07.057>.
- Shi J, Zhou Y, Huang H-C, and Mitchison TJ (2011). Navitoclax (ABT-263) accelerates apoptosis during drug-induced mitotic arrest by antagonizing Bcl-xL. *Cancer Res* **71**, 4518–4526. <https://doi.org/10.1158/0008-5472.CAN-10-4336>.
- Bah N, Maillat L, Ryan J, Dubreil S, Gautier F, Letai A, Juin P, and Barillé-Nion S (2014). Bcl-xL controls a switch between cell death modes during mitotic arrest. *Cell Death Dis* **5**e1291. <https://doi.org/10.1038/cddis.2014.251>.
- Shoemaker AR, Oleksijew A, Bauch J, Belli BA, Borre T, Bruncko M, Deckwirth T, Frost DJ, Jarvis K, and Joseph MK, et al (2006). A small-molecule inhibitor of Bcl-X<sub>L</sub> potentiates the activity of cytotoxic drugs *in vitro* and *in vivo*. *Cancer Res* **66**, 8731–8739. <https://doi.org/10.1158/0008-5472.CAN-06-0367>.
- Wong M, Tan N, Zha J, Peale FV, Yue P, Fairbrother WJ, and Belmont LD (2012). Navitoclax (ABT-263) reduces Bcl-x(L)-mediated chemoresistance in ovarian cancer models. *Mol Cancer Ther* **11**, 1026–1035. <https://doi.org/10.1158/1535-7163.MCT-11-0693>.
- Tan N, Malek M, Zha J, Yue P, Kassees R, Berry L, Fairbrother WJ, Sampath D, and Belmont LD (2011). Navitoclax enhances the efficacy of taxanes in non-small cell lung cancer models. *Clin Cancer Res* **17**.
- Eischen CM, Woo D, Roussel MF, and Cleveland JL (2001). Apoptosis triggered by myc-induced suppression of Bcl-X<sub>L</sub> or Bcl-2 is bypassed during lymphomagenesis. *Mol Cell Biol* **21**, 5063–5070. <https://doi.org/10.1128/MCB.21.15.5063>.
- Maclean KH, Keller UB, Rodriguez-Galindo C, Nilsson JA, and Cleveland JL (2003). c-Myc augments gamma irradiation-induced apoptosis by suppressing Bcl-X<sub>L</sub>. *Mol Cell Biol* **23**, 7256–7270. <https://doi.org/10.1128/MCB.23.20.7256-7270.2003>.
- Huntzinger E and Izaurralde E (2011). Gene silencing by microRNAs: contributions of translational repression and mRNA decay. *Nat Rev Genet* **12**, 99–110. <https://doi.org/10.1038/nrg2936>.
- Lu J, Getz G, Miska EA, Alvarez-Saavedra E, Lamb J, Peck D, Sweet-Cordero A, Ebert BL, Mak RH, and Ferrando AA, et al (2005). MicroRNA expression profiles classify human cancers. *Nature* **435**, 834–838. <https://doi.org/10.1038/nature03702>.
- Pollari S, Käkönen S-M, Edgren H, Wolf M, Kohonen P, Sara H, Guise T, Nees M, and Kallioniemi O (2011). Enhanced serine production by bone metastatic breast cancer cells stimulates osteoclastogenesis. *Breast Cancer Res Treat* **125**, 421–430. <https://doi.org/10.1007/s10549-010-0848-5>.
- Bennett A, Sloss O, Topham C, Nelson L, Tighe A, and Taylor SS (2016). Inhibition of Bcl-xL sensitizes cells to mitotic blockers, but not mitotic drivers. *Open Biol* **6**, 160134. <https://doi.org/10.1098/rsob.160134>.
- Pruikkonen S and Kallio MJ (2017). Excess of a Rassf1-targeting microRNA, miR-193a-3p, perturbs cell division fidelity. *Br J Cancer* **116**, 1451–1461. <https://doi.org/10.1038/bjc.2017.110>.
- Wellner U, Schubert J, Burk UC, Schmalhofer O, Zhu F, Sonntag A, Waldvogel B, Vannier C, Darling D, and zur Hausen A, et al (2009). The EMT-activator

- ZEB1 promotes tumorigenicity by repressing stemness-inhibiting microRNAs. *Nat Cell Biol* **11**, 1487–1495. <https://doi.org/10.1038/ncb1998>.
- [27] Mäki-Jouppila JHE, Pruikkonen S, Tambe MB, Aure MR, Halonen T, Salmela AL, Laine L, Børresen-Dale AL, and Kallio MJ (2015). MicroRNA let-7b regulates genomic balance by targeting Aurora B kinase. *Mol Oncol* **9**, 1056–1070.
- [28] Koboldt DC, Fulton RS, McLellan MD, Schmidt H, Kalicki-Veizer J, McMichael JF, Fulton LL, Dooling DJ, Ding L, and Mardis ER, et al (2012). Comprehensive molecular portraits of human breast tumours. *Nature* **490**, 61–70. <https://doi.org/10.1038/nature11412>.
- [29] Tambe M, Pruikkonen S, Mäki-Jouppila J, Chen P, Elgaen BV, Straume AH, Huhtinen K, Cárpen O, Lønning PE, and Davidson B, et al (2016). Novel Mad2-targeting miR-493-3p controls mitotic fidelity and cancer cells' sensitivity to paclitaxel. *Oncotarget* **7**, 12267–12285. <https://doi.org/10.18632/oncotarget.7860>.
- [30] Chrisanthar R, Knappskog S, Løkkevik E, Anker G, Østenstad B, Lundgren S, Risberg T, Mjaaland I, Skjønberg G, and Aas T, et al (2011). Predictive and prognostic impact of TP53 mutations and MDM2 promoter genotype in primary breast cancer patients treated with epirubicin or paclitaxel. *PLoS One* **6**e19249. <https://doi.org/10.1371/journal.pone.0019249>.
- [31] Chrisanthar R, Knappskog S, Løkkevik E, Anker G, Østenstad B, Lundgren S, Berge EO, Risberg T, Mjaaland I, and Maehle L, et al (2008). CHEK2 mutations affecting kinase activity together with mutations in TP53 indicate a functional pathway associated with resistance to epirubicin in primary breast cancer. *PLoS One* **3**e3062. <https://doi.org/10.1371/journal.pone.0003062>.
- [32] Love MI, Huber W, and Anders S (2014). Moderated estimation of fold change and dispersion for RNA-seq data with DESeq2. *Genome Biol* **15**, 550. <https://doi.org/10.1186/s13059-014-0550-8>.
- [33] Barbosa-Morais NL, Dunning MJ, Samarajiwa SA, Darot JFJ, Ritchie ME, Lynch AG, and Tavaré S (2010). A re-annotation pipeline for Illumina BeadArrays: improving the interpretation of gene expression data. *Nucleic Acids Res* **38**e17. <https://doi.org/10.1093/nar/gkp942>.
- [34] Bolstad BM, Irizarry RA, Astrand M, and Speed TP (2003). A comparison of normalization methods for high density oligonucleotide array data based on variance and bias. *Bioinformatics* **19**, 185–193. <http://www.ncbi.nlm.nih.gov/pubmed/12538238>, Accessed date: 5 July 2017.
- [35] Chang T-C, Yu D, Lee Y-S, Wentzel EA, Arking DE, West KM, Dang CV, Thomas-Tikhonenko A, and Mendell JT (2008). Widespread microRNA repression by Myc contributes to tumorigenesis. *Nat Genet* **40**, 43–50. <https://doi.org/10.1038/ng.2007.30>.
- [36] Li J, Chen Y, Zhao J, Kong F, and Zhang Y (2011). miR-203 reverses chemoresistance in p53-mutated colon cancer cells through downregulation of Akt2 expression. *Cancer Lett* **304**, 52–59. <https://doi.org/10.1016/j.canlet.2011.02.003>.
- [37] Consortium EP (2012). An integrated encyclopedia of DNA elements in the human genome. *Nature* **489**, 57–74. <https://doi.org/10.1038/nature11247>.
- [38] Pelengaris S, Khan M, and Evan G (2002). c-MYC: more than just a matter of life and death. *Nat Rev Cancer* **2**, 764–776. <https://doi.org/10.1038/nrc904> [pii].
- [39] Adams CM and Eischen CM (2016). Histone deacetylase inhibition reveals a tumor-suppressive function of MYC-regulated miRNA in breast and lung carcinoma. *Cell Death Differ* **23**, 1312–1321. <https://doi.org/10.1038/cdd.2016.9>.
- [40] Adams CM, Hiebert SW, and Eischen CM (2016). Myc induces miRNA-mediated apoptosis in response to HDAC inhibition in hematologic malignancies. *Cancer Res* **76**, 736–748. <https://doi.org/10.1158/0008-5472.CAN-15-1751>.
- [41] Jordan MA, Wendell K, Gardiner S, Derry WB, Copp H, and Wilson L (1996). Mitotic block induced in HeLa cells by low concentrations of paclitaxel (Taxol) results in abnormal mitotic exit and apoptotic cell death. *Cancer Res* **56**, 816–825. <http://www.ncbi.nlm.nih.gov/pubmed/8631019>, Accessed date: 10 February 2017.
- [42] Xu W-S, Perez G, Ngo L, Gui C-Y, and Marks PA (2005). Induction of polyploidy by histone deacetylase inhibitor: a pathway for antitumor effects. *Cancer Res* **65**. <http://cancerres.aacrjournals.org/content/65/17/7832.long>, Accessed date: 7 February 2018.
- [43] Oakes SR, Vaillant F, Lim E, Lee L, Breslin K, Feleppa F, Deb S, Ritchie ME, Takano E, and Ward T, et al (2012). Sensitization of BCL-2-expressing breast tumors to chemotherapy by the BH3 mimetic ABT-737. *Proc Natl Acad Sci U S A* **109**, 2766–2771. <https://doi.org/10.1073/pnas.1104778108>.
- [44] Wali VB, Langdon CG, Held MA, Platt JT, Patwardhan GA, Safonov A, Aktas B, Pusztai L, Stern DF, and Hatzis C (2017). Systematic drug screening identifies tractable targeted combination therapies in triple-negative breast cancer. *Cancer Res* **77**. <https://doi.org/10.1158/0008-5472.CAN-16-1901>.